LASER & PHOTONICS REVIEWS

www.lpr-journal.org

Low-Threshold Lasing from Copper-Doped CdSe Colloidal Quantum Wells

Junhong Yu, Manoj Sharma, Mingjie Li, Savas Delikanli, Ashma Sharma, Muhammad Taimoor, Yemliha Altintas, James R. McBride, Thomas Kusserow, Tze-Chien Sum, Hilmi Volkan Demir, and Cuong Dang**

Transition metal doped colloidal nanomaterials (TMDCNMs) have recently attracted attention as promising nano-emitters due to dopant-induced properties. However, despite ample investigations on the steady-state and dynamic spectroscopy of TMDCNMs, experimental understandings of their performance in stimulated emission regimes are still elusive. Here, the optical gain properties of copper-doped CdSe colloidal quantum wells (CQWs) are systemically studied with a wide range of dopant concentration for the first time. This work demonstrates that the amplified spontaneous emission (ASE) threshold in copper-doped CQWs is a competing result between the biexciton formation, which is preferred to achieve population inversion, and the hole trapping which stymies the population inversion. An optimum amount of copper dopants enables the lowest ASE threshold of ≈7 μJ cm^{-2}, about 8-fold reduction from that in undoped CQWs (≈58 μJ cm^{-2}) under sub-nanosecond pulse excitation. Finally, a copper-doped CQW film embedded in a vertical cavity surface-emitting laser (VCSEL) structure yields an ultralow lasing threshold of 4.1 μJ cm^{-2}. Exploiting optical gain from TMDCNMs may help to further boost the performance of colloidal-based lasers.

1. Introduction

Transition metal doped colloidal nanomaterials (TMDCNMs), including Cu, Ag, and Mn, have recently attracted broad interest for optoelectronic applications.[1–3] Compared with their undoped counterparts, TMDCNMs not only retain all the advantages of the host colloidal nanomaterials but also exhibit novel optical/electronic properties introduced by transition metal ions, such as a broadband Stokes-shifted emission,[4] p-type conductivity,[5] and photoinduced magnetism resulting from spin-exchange interaction.[6] Extensive progress about TMDCNMs has been reported over the past several years. From the perspective of fundamental understanding, the role of dopants in the bandgap modulation and steady-state/transient photoluminescence (PL) has been investigated into great

Dr. J. Yu, Dr. M. Sharma, Dr. S. Delikanli, A. Sharma, Prof. H. V. Demir, Prof. C. Dang
LUMINOUS! Centre of Excellence for Semiconductor Lighting and Displays
School of Electrical and Electronic Engineering
The Photonics Institute (TPI)
Nanyang Technological University
50 Nanyang Avenue, 639798 Singapore
E-mail: volkan@stanfordalumni.org; hcdang@ntu.edu.sg

Dr. M. Li, Prof. T.-C. Sum, Prof. H. V. Demir
School of Physical and Mathematical Sciences
Nanyang Technological University
639798 Singapore

Dr. S. Delikanli, Dr. Y. Altintas, Prof. H. V. Demir
Department of Electrical and Electronics Engineering and Department of Physics
UNAM-Institute of Materials Science and Nanotechnology
Bilkent University
Bilkent, Ankara 06800, Turkey

Dr. M. Taimoor, Prof. T. Kusserow
Institute of Nanostructure Technologies and Analytics/CINSaT
University of Kassel
Heinrich-Plett-Str. 40, Kassel 34132, Germany

Dr. Y. Altintas
Department of Material Science and Nanotechnology Engineering
Abdullah Gul University
Kayseri 38080, Turkey

Prof. J. R. McBride
Department of Chemistry and Vanderbilt Institute for Nanoscale Science and Engineering
Vanderbilt University
Nashville, Tennessee 37235, United States

Prof. C. Dang
CINTRA UMI CNRS/NTU/THALES 3288
Research Techno Plaza
50 Nanyang Drive, Border X Block, Level 6, 637553 Singapore

The ORCID identification number(s) for the author(s) of this article can be found under https://doi.org/10.1002/lpor.202100034

DOI: 10.1002/lpor.202100034

depth.[5,7–11] From the perspective of application, benefiting from the nearly zero self-absorption in the dopant related emission, Sharma et al. demonstrated near-unity photoluminescence quantum yields in the luminescent solar concentrators using copper-doped colloidal quantum wells (CQWs).[4]

To date, majority of the works on TMDCNMs are conducted with low pump fluence/intensity (i.e., stay in the sub-single/single exciton regime) and the potential of TMDCNMs as optical gain materials has not aroused much attention. There is a current belief that TMDCNMs are awful emitters to achieve the stimulated emission since dopants typically behave as the hole-trappers which severely hinder the built-up of population inversion in the host.[12,13] However, this argument does not consider the effect of dopants on the excitonic dynamics of the host. For example, dopants can enhance the quantum yield to near unity in colloidal nanomaterials via suppressing the intrinsic defects.[4,10] Also, dopants localize the holes and offer the chance to form trapped excitons in the host; the trapped excitons with higher oscillator strength can interact with each other heavily to form the high-order excitonic states and facilitate the population inversion.[14,15] Moreover, trapping holes also modify the Coulomb environment in the host and it is possible that the suppressed Coulomb screening effect[16,17] helps the onset of stimulated emission. Therefore, it is worthwhile to investigate the optical gain performance in TMDCNMs.

Here, through analyzing the amplified spontaneous emission (ASE) spectra in copper-doped CdSe CQWs with varying amount of copper dopants, we observe that copper dopants enable the CQWs exhibiting biexciton emission with strong biexciton binding energy (≈64 meV) under extremely low pump fluence (<1 μJ cm^{-2}). As a result, the ASE threshold in copper-doped CQWs is the result of a competition between two opposite effects: biexciton formation which facilitates the population inversion and hole trapping which stymies the population inversion. At the copper dopant level of ≈40 per CQW, the ASE threshold in copper-doped CQWs has been reduced by eight times compared to the value in undoped CQWs (≈7 μJ cm^{-2} versus ≈58 μJ cm^{-2}). To further access the biexcitonic gain potential of copper-doped CQWs, we have demonstrated a vertical cavity surface emitting laser (VCSEL) and an ultralow threshold of ≈4 μJ cm^{-2} is achieved under sub-nanosecond excitation, a value comparable to or lower than those reported colloidal nanomaterial based lasing devices.[18–20]

2. Results and Discussion

We prepare the copper-doped and undoped 4-monolayer CdSe CQWs according to the existing recipes[4,7] and optimize the procedures to achieve copper-doped CQWs with high aspect ratio to avoid stacking (details of the modified recipes are described in Note S1, Supporting Information). For the optical gain study, the amount of copper dopants is controlled by the volume of copper precursor added; and the average number of copper dopants per CQW, $\langle N_{Cu} \rangle$, is determined by the inductively coupled plasma mass spectrometry (ICP:MS, see details in the Experimental Section).[4] An example of the steady-state optical properties of doped and undoped CQWs under UV illumination is shown in **Figure 1**a (we only display the PL and absorption of doped sample with ≈40 copper dopants per CQW, the spectra of other doping level are shown in Figure S1, Supporting Information), the similar absorption spectra indicate that excitonic resonance in CQW host is not affected by copper dopants. Notably, besides showing a narrow band-edge emission (BE), doped CQWs display a broad PL band at the low energy side, which is called the copper-related emission (CE). As shown in Figure 1b, CE is attributed to the recombination between the captured holes in copper dopants and the electrons in the conduction band (CB) of the host CQWs: $Cu^{2+} + e \rightarrow Cu^{1+} + h\nu$ ($h\nu$ is the photon energy of CE and e denotes an electron in CB).[4,5,21] The BE dynamics of doped (green circles) and undoped (black squares) CQWs in solution with low pump fluence (<0.1 μJ cm^{-2}) is presented in Figure 1c. In the short-time window (up to 400 ps), the ultrafast recombination channel (≈31 ps) in undoped CQWs is absent in copper-doped CQWs. The single exponential decay behavior of copper-doped CQWs is consistent with theoretical calculation conducted by Nelson,[10] in which highly localized covalent [$CuSe_4$] cluster can suppress intrinsic traps (structure defects) and thus, enhance the PL quantum yield (PLQY) of copper-doped nanocrystals. Moreover, the reduced lifetime of copper-doped CQWs both in the short-time window and the long-time window (up to 4 ns) suggest that copper dopants are trapping holes from the host.

To investigate the ASE behavior of copper-doped CQWs, we prepared a close-packed solid film by drop-casting then used stripe excitation geometry with sub-nanosecond pulse laser for pumping (see the details of ASE measurement in the Experimental Section). We compared the emission properties between undoped and copper-doped CQWs to understand the effect of dopants. A color-coded map of ASE spectra for undoped sample is presented in **Figure 2**a (the corresponding 1D spectra is shown in Figure S2, Supporting Information), a narrowing emission spectrum is observed when the pump fluence is beyond the ASE threshold of ≈58 μJ cm^{-2}, which is typical as reported previously.[22–24] For doped sample with ≈40 copper dopants per CQW, as shown in the color-coded map of ASE spectra in Figure 2b (the corresponding 1D spectra is presented in Figure S3, Supporting Information), when excitation fluence is low (< 0.1 μJ cm^{-2}), BE spectra are symmetric and peak at ≈514 nm. As the fluence increases but still below the ASE threshold, a new emission channel appears to broaden the BE spectra and is assigned as the biexciton emission because of the superlinear intensity increase compared to the exciton emission (see the left panel of Figure 2c, more evidences for the biexciton justification can be found in our previous work).[24] With the fluence higher than ≈0.22 μJ cm^{-2} (the bottom white dashed line in Figure 2b), biexciton emission becomes the strongest emission channel. When the fluence is even stronger, beyond ≈7.05 μJ cm^{-2}, ASE emerges with a sharp increase of BE intensity and the narrowing of the BE spectra (FWHM: ≈8 nm, see the right panel of Figure 2c). Meanwhile, CE starts to saturate when excitation is reaching the ASE threshold (as indicated by the white dashed line in the right panel of Figure 2b). This observation is another evidence to support that copper dopants are consuming the excitation energy in the CQW host via hole trapping and ASE can only happen when copper dopants are fulfilled. In summary, there are two opposite effects which can influence the ASE behavior in copper-doped CQWs: (1) the strong biexciton emission which supports population inversion due to the formation of a four-energy-level system;[25,26] (2) the

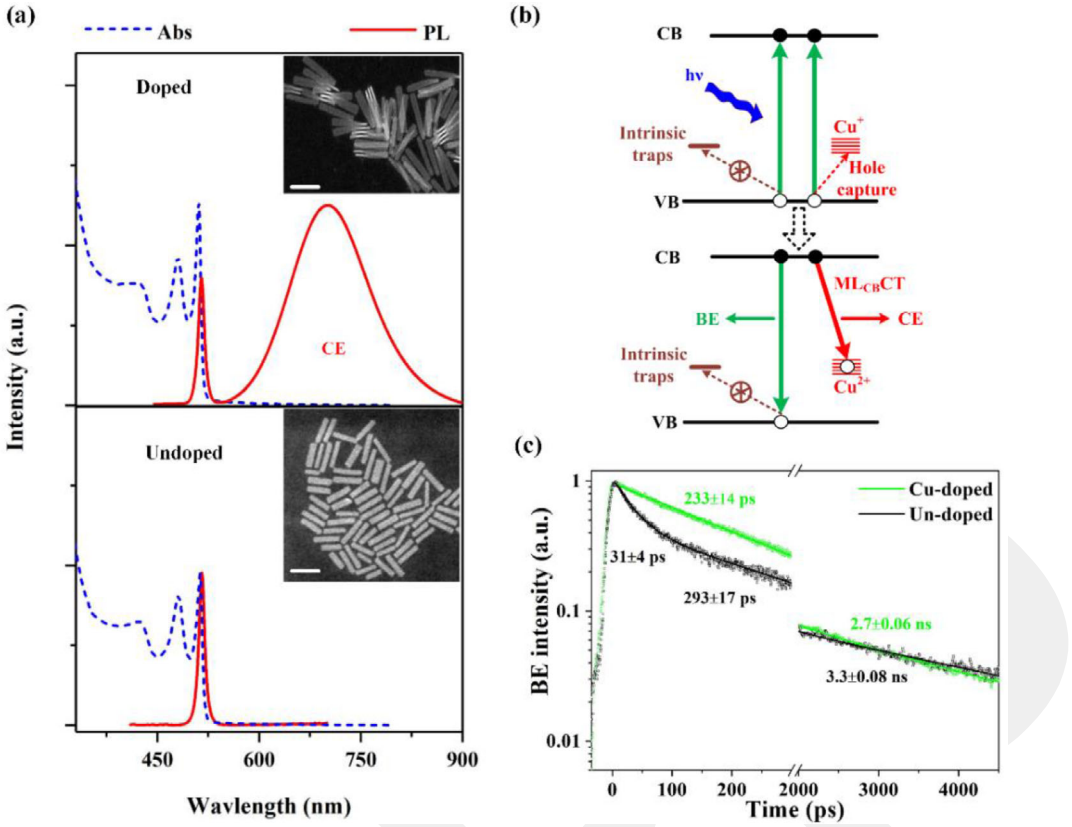

Figure 1. Optical properties of undoped and copper-doped colloidal quantum wells (CQWs). a) The steady-state optical properties of undoped (bottom) and copper-doped (top) CQWs. The insets are the high-angle annular dark-field scanning transmission electron microscopy (HAADF-STEM) images (scale bar: 30 nm). The copper-doped CQWs display two emission bands: band-edge emission (BE) and copper-related emission (CE). b) The schematics to illustrate the carrier transitions and radiative recombination in copper-doped CQWs. c) Normalized decay curves of BE for undoped CQWs (measurement: black square; fitting: black solid line) and copper-doped CQWs (measurement: green circle; fitting: green solid line) with the low pump fluence, the photoluminescence (PL) dynamics of both doped and undoped CQWs are probed at 514 nm in hexane.

hole trapping which becomes a dopant-induced loss channel and damages the population inversion in the host by filling the valence band (i.e., capturing holes). And we speculate that the lowest ASE threshold in copper-doped CQWs should be with optimum dopant level to not only take the advantage of biexciton formation but also reduce adverse effect from hole trapping.

To verify our speculation, we have conducted ASE measurement in copper-doped CQWs with different amounts of dopants. The threshold result is summarized in **Figure 3** together with the CE fraction percentage which is an optical indication of doping level. The CE fraction percentage is calculated from emission spectra of doped samples under the UV-lamp illumination (see Figure S1, Supporting Information). Three zones can be observed for the copper-doped samples with different dopant levels. In zone I (i.e., light doping: $\langle N_{Cu} \rangle$ is smaller than 10), copper-doped CQWs display a low PLQY (≈30%, which is comparable with the undoped CQWs) associated with a small CE fraction percentage.[4,7] In this zone, threshold is higher than that in undoped CQWs since the biexciton emission is not well-separated from exciton transition and hole trapping degrades the ASE performance (see the ASE spectra in Figure S4, Supporting Information). With further increasing the dopant precursor amount (i.e., medium doping: $\langle N_{Cu} \rangle$ is in the range 10–40) in zone II, the PLQY becomes higher than that in zone I due to the suppression of defects as discussed in Figure 1. These dopant levels are significant enough to ease the biexciton formation and make a large red shift of biexciton emission from exciton transition. These advantages dominate the adverse hole trapping effect to decrease the ASE threshold, reaching the lowest value of ≈7 μJ cm^{-2} when $\langle N_{Cu} \rangle$ is around 40 (as shown in Figure 2 and Figure S3, Supporting Information). Furthermore, in zone III (i.e., heavy doping: $\langle N_{Cu} \rangle$ is larger than 40), we have achieved the highest PLQY. However, the CE is overwhelming the emission spectrum (CE percentage > 99%), implying that a huge portion of excitation energy is lost due to hole trapping. Consequently, the optical gain performance becomes poor again with increase ASE threshold substantially (see also the ASE spectra in Figure S5, Supporting Information). It is worth to note that though the PLQY is very high but most of emission is from CE, which is considered as loss for population build up at the band edge.

A VCSEL is a good testbed for us to demonstrate the lasing performance in copper-doped CQWs.[17] We use the copper-doped CQWs with the best ASE performance (i.e., 40 cooper dopants per CQW) and a typical structure of the VCSEL device as shown in **Figure 4**a: a spin-casted copper-doped CQW film is embedded in a planar cavity constructed from two Bragg mirrors

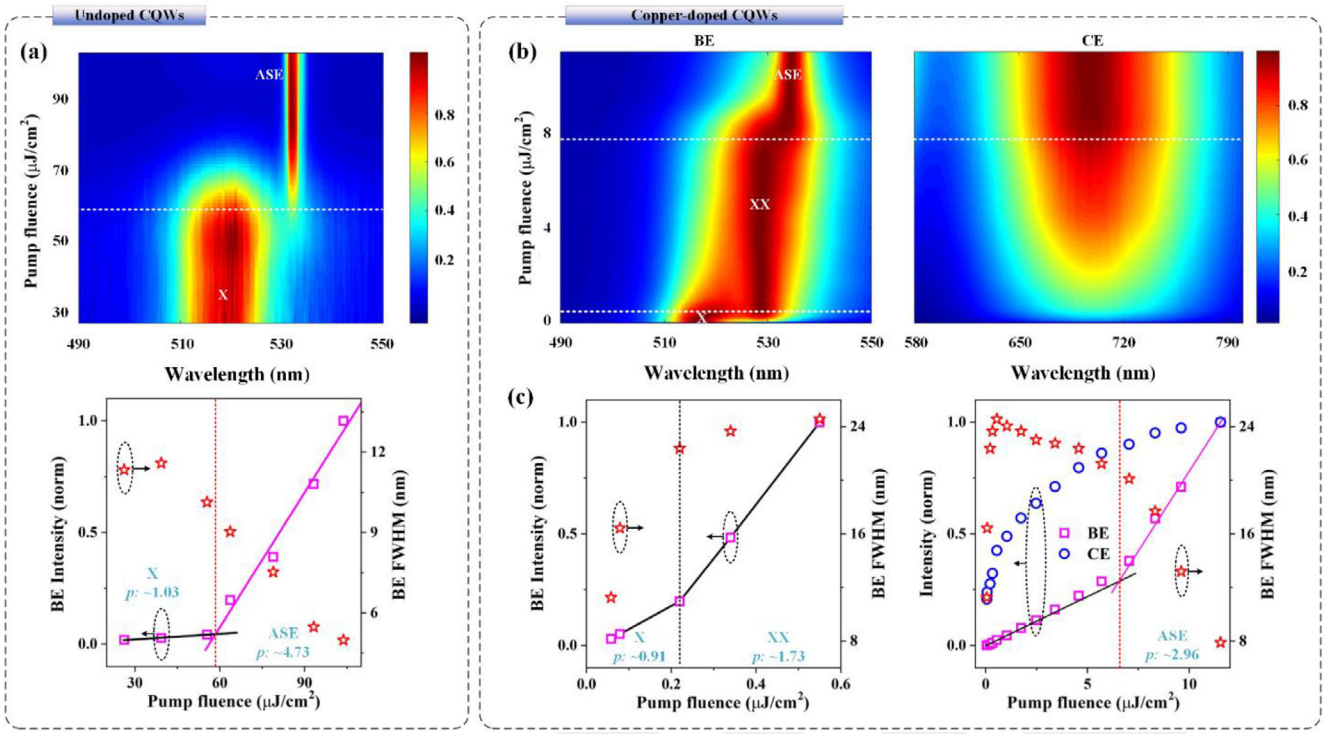

Figure 2. Amplified spontaneous emission (ASE) in undoped and copper-doped colloidal quantum wells (CQWs) under the excitation of sub-nanosecond laser pulses. a) Upper panel: 2D spectra map for undoped CQWs, the map is normalized by the maximum emission intensity at each fluence. Lower panel: integrated emission intensity (magenta squares) and FWHM (red stars) for undoped CQWs. The ASE threshold of ≈58.4 μJ cm^{-2} is extracted. b) 2D spectra map for copper-doped CQWs. Left panel: Band-edge emission (BE) normalized by the maximum BE intensity at each fluence. Right panel: Copper-related emission (CE) normalized by the maximum CE intensity at the highest fluence. X: exciton emission. XX: biexciton emission. The dashed white lines point out the onset of biexciton emission and ASE, respectively. c) Left panel: Integrated BE intensity (magenta squares) and FWHM of BE (red stars) for copper-doped CQWs with low pump fluence. Beyond ≈0.22 μJ cm^{-2}, biexcitons emission dominates the BE; Right panel: Integrated BE intensity (magenta squares), CE intensity (blue circles), and FWHM of BE (red stars) for copper-doped CQWs with high pump fluence. The ASE threshold of ≈7.05 μJ cm^{-2} is extracted. The straight lines in lower row plots are to guide our eyes and to find the onset points of biexciton and ASE. The intensity (I) from different emission mechanism is fitted as a function of excitation fluence (F) using the power-law formula: $I = aF^p$ (a and p are the fitting parameters). The p value is shown in the figure.

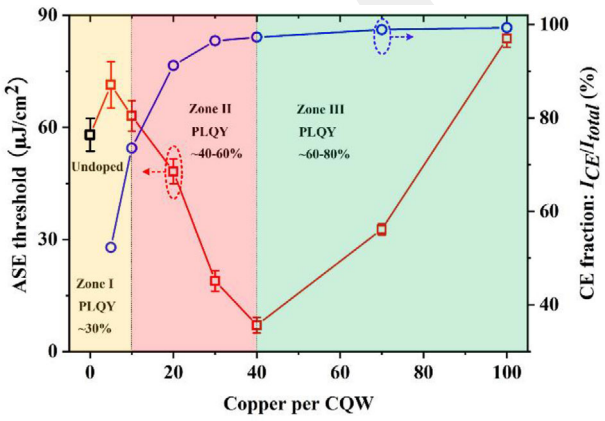

Figure 3. The effect of copper dopants on amplified spontaneous emission (ASE) threshold: Variation of ASE thresholds for copper-doped colloidal quantum wells (CQWs) with different amounts of dopants per CQW. Copper-related emission (CE) fraction of the emission spectra under UV illumination with respect to total integrated emission, $I_{CE}/(I_{CE}+I_{BE})$, has been co-plotted along with ASE thresholds. Quantum yield numbers are also listed.

(see the reflection spectra of Bragg mirrors in Figure S6, Supporting Information). The VCSEL with copper-doped CQW gain media is excited by a focused laser spot with a diameter of 15 μm and the emission is collected coaxially on the reflection side at the normal direction. It is worth pointing out that the cavity length in our VCSEL is controlled by a differential micrometer drive (see the Experimental Section for details) and that both single-mode (shown in Figure 4) and multiple-mode lasing (see Figure S6, Supporting Information) are demonstrated. Figure 4b depicts the logarithmic plot of emission intensities with different fluences. We notice that the spontaneous emission in VCSEL is red-shifted compared to the ASE measurement, which is probably due to density of states modification by a dielectric cavity.[18] When fluence is high enough, a narrow single-mode lasing peak (≈531 nm) is observed, as shown in the pseudo-color intensity map (see Figure 4c). The lasing action is further demonstrated by the spectra analysis (see Figure 4d): the integrated BE intensity clearly exhibits an S-shape nonlinear dependence and FWHM of BE shrinks from ≈12 down to ≈0.3 nm when the fluence exceeds ≈4.13 μJ cm^{-2}, suggesting the transition from spontaneous emission to lasing. In addition, after crossing the lasing threshold, as shown in Figure 4e, a high-brightness spot significantly

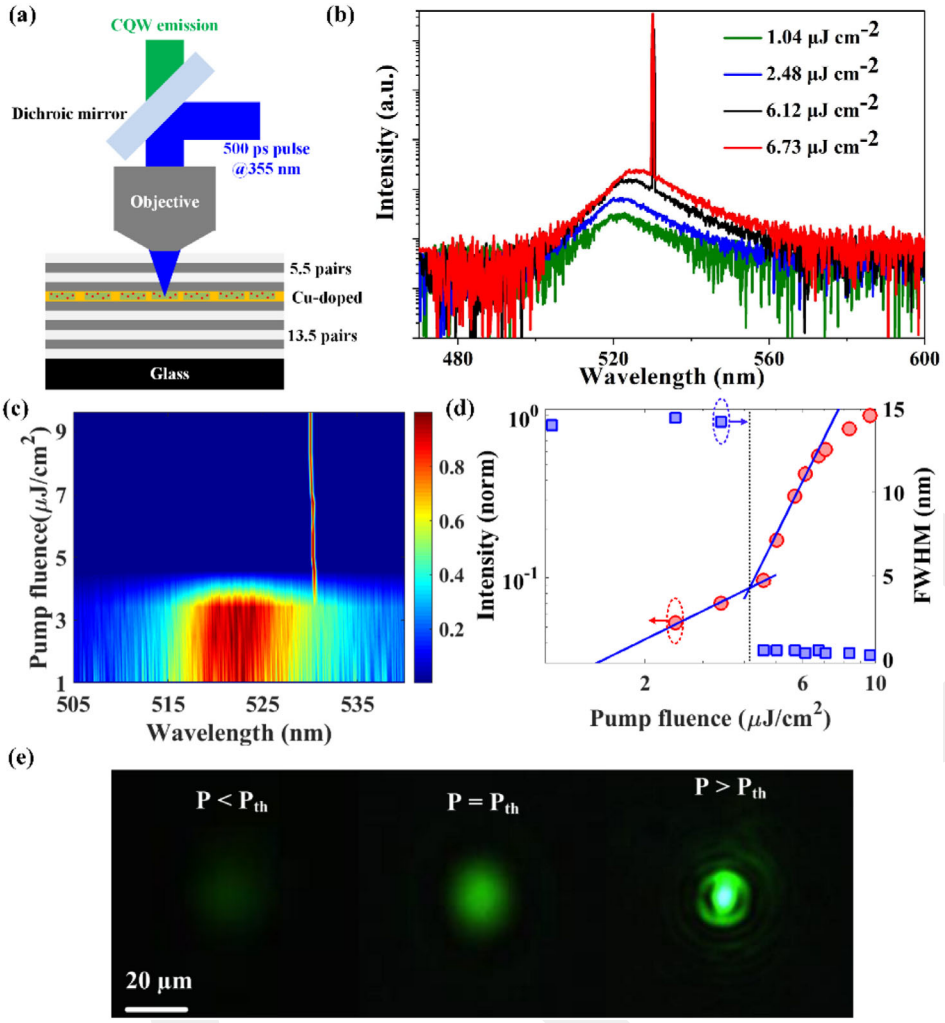

Figure 4. Vertical cavity surface-emitting laser (VCSEL) with copper-doped colloidal quantum well (CQW) gain media under the excitation of sub-nanosecond laser pulse. a) Schematic of the VCSEL with two distributed Bragg reflectors (DBR, reflectivity at 525–535 nm > 99%). b) Emission spectra of band-edge emission (BE) in VCSEL with varied fluences on a semi-logarithmic plot, demonstrating single-mode lasing. c) The normalized spectral map of BE in VCSEL, showing the transition from a spectrally broad spontaneous emission to a sharp lasing peak. d) The integrated BE intensity (red circle) with increasing fluence in a log–log scale, showing a clear knee behavior. Blue lines are the log–log fitting of BE intensity, extracting a lasing threshold of ≈4.1 μJ cm^{-2}. Blue squares show the change of FWHM of BE as a function of the fluence. e) Emission images of VCSEL when the excitation fluence is below, near, and beyond the lasing threshold.

different from dim, broad spontaneous emission indicates the well-defined spatial coherence in our VCSEL device.[18–20]

3. Conclusion

In summary, we have studied the optical gain performance of copper-doped CdSe CQWs with varying amount of copper dopants. The pump-fluence-dependent PL spectra of the solid film indicate that an optimum copper amount (≈40 dopants per CQW on average) can facilitate the biexciton formation and significantly lower the ASE threshold in CdSe CQWs despite the dopants consume the excitonic energy in the host via hole trapping. Using the optimized copper-doped CQWs as the gain material, excellent lasing performance with the threshold as low as 4.1 μJ cm^{-2} in the VCSEL device comprising of two distributed Bragg reflectors has been demonstrated. Future efforts following this study lie in the physical understanding of the copper's role on the biexcitons in CdSe host including the formation mechanism and the constituent of biexcitons.

4. Experimental Section

Estimating the Cu Atomic Level: With inductively coupled plasma mass spectrometry (ICP:MS) we estimated Cu atomic levels with respect to cadmium and selenium. Average dimensions of our 4 ML copper-doped CdSe CQWs measured by TEM microscopy were (50.2 ± 1.1) × (8.0 ± 1.2) × 1.2 nm, which suggest 9900 cadmium and 7800 selenium atoms in one CQW. Therefore, using ICP:MS measurements we can estimate Cu atoms per CQW.

Steady-State Optical Characterization of Copper-Doped and Undoped CQWs: Absorption spectra CQWs in hexane (both doped and undoped

CQWs are 10^{-4} mol mL^{-1}) were measured by a UV–VIS spectrophotometer (Shimadzu, UV-1800). PL spectra of CQWs in hexane (both doped and undoped CQWs are 10^{-4} mol mL^{-1}) were recorded using a spectrofluorophotometer (Shimadzu, RF-5301PC, excitation wavelength: 355 nm). Quantum yield (QY) of CQWs in hexane (both doped and undoped CQWs are 10^{-2} mol mL^{-1}) was measured with an integrating sphere and calculated as the ratio of absolute emission and absorption photons. The accuracy of the QY measurement was verified using Rhodamine 6G, whose QY of 94.3% measured in our setup, is found in good agreement with the standard value of 95%.

Time-Resolved Photoluminescence Measurement: Time-resolved PL (TRPL) measurements were performed with a streak camera from Optronics. The 400-nm pump laser pulses for TRPL were generated from a 1000 Hz regenerative amplifier (Coherent LibraTM). The beam from the regenerative amplifier had a center wavelength at 800 nm, a pulse width of around 150 fs, and was seeded by a mode-locked Ti-sapphire oscillator (Coherent Vitesse, 80MHz). A 400-nm pump laser was obtained by frequency doubling the 800-nm fundamental regenerative amplifier output using a BBO crystal. All measurements were performed in the solid film at room temperature in ambient air (53 ± 2% humidity) conditions.

Amplified Spontaneous Emission Measurement: The pump laser at 355 nm used for stripe excitation in the ASE measurement was a frequency tripling of Nd:YAG laser with a pulse width of 0.5 ns and a repetition rate of 100 Hz. The laser beam was focused onto a stripe along the drop-casted film on the glass substrate using a cylindrical lens. The width of the stripe, which contains (1 – 1/e) of the power in the laser beam, was 50 µm, determined using the knife-edge method. In the experiment, the stripe length was 4 mm. An automatically rotated $\lambda/4$ waveplate (WPQ05M-532, THORLABS) and polarizer (CCM1-WPBS254, THORLABS) were used to adjust the pump fluence. Then, the emission was collected via a fiber-coupled ANDOR spectrometer (monochromator: ANDOR Shamrock 303i, CCD: ANDOR iDus 401). The collection geometry was perpendicular to the laser pump. All measurements were performed at room temperature in air.

Vertical-Cavity Surface-Emitting Laser: Two kinds of DBRs with 5.5 (top DBR) and 13.5 (bottom DBR) periods of alternating $\lambda/4$ layers of Nb_2O_5/SiO_2 were fabricated using ion beam sputter deposition (IBSD) leading to a stop-band width of 140 nm around the emission wavelength and R_{max} >99%. As the optical gain medium, copper-doped CQW film was deposited on the surface of one DBR at a spin-rate of 2000 rpm for 60 s using a concentrated solution (20 mg mL^{-1} in hexane). Then, a differential micrometer drive (DM22, THORLABS, the smallest incremental move: 50 nm) was used to push the second DBR close to the CQW film, also controlled the cavity optical length to achieve single-mode or multimode lasing. All measurements were performed in the reflection geometry at room temperature in air and using the same laser pulse as described in the ASE measurement.

Supporting Information

Supporting Information is available from the Wiley Online Library or from the author.

Acknowledgements

The authors would like to acknowledge the financial support from Singapore National Research Foundation under the Program of NRF-NRFI2016-08, the Competitive Research Program NRF-CRP14-2014-03 and Singapore Ministry of Education AcRF Tier-1 grant (MOE2019-T1-002-087). H.V.D is also grateful to acknowledge additional financial support from the TUBA.

Author Contributions

J.Y., M.S. and M.L. contributed equally to this work. C.D. and H.V.D. supervised and contributed to all aspects of the research. J.Y., M.S., H.V.D. and C.D. wrote the manuscript. J.Y. conducted the spectroscopy measurement and VCSEL fabrication. M.S. performed the material synthesis and designed them to achieve the best biexciton lasing performance. S.D. and A.S. helped in material synthesis and characterizations. M.L. performed transient PL dynamics measurement. M.L. and TC.S. supervised the ultrafast dynamics analysis. Y.A. and J.R.M. conducted the material characterization. M.T. and T.K. fabricated the Bragg mirrors and proposed the tuning cavity. All authors analyzed the data, discussed the results, commented on the manuscript, and participated in manuscript revision.

Conflict of Interest

The authors declare no conflict of interest.

Data Availability Statement

The data that support the findings of this study are available from the corresponding author upon reasonable request.

Keywords

amplified spontaneous emission, colloidal quantum wells, copper doping, lasing, vertical cavity surface-emitting lasers

Received: January 23, 2021
Revised: March 8, 2021
Published online: May 4, 2021

[1] D. J. Norris, A. L. Efros, S. C. Erwin, *Science* **2008**, *319*, 1776.
[2] S. C. Erwin, L. Zu, M. I. Haftel, A. L. Efros, T. A. Kennedy, D. J. Norris, *Nature* **2005**, *436*, 91.
[3] D. J. Norris, Yao, N., Charnock, F. T., Kennedy, T. A., *Nano Lett.* **2001**, *1*, 3.
[4] M. Sharma, K. Gungor, A. Yeltik, M. Olutas, B. Guzelturk, Y. Kelestemur, T. Erdem, S. Delikanli, J. R. McBride, H. V. Demir, *Adv. Mater.* **2017**, *29*, 1700821.
[5] K. E. Hughes, K. H. Hartstein, D. R. Gamelin, *ACS Nano* **2018**, *12*, 718.[CrossRef]
[6] S. T. Ochsenbein, Y. Feng, K. M. Whitaker, E. Badaeva, W. K. Liu, X. Li, D. R. Gamelin, *Nat. Nanotechol.* **2009**, *4*, 681.
[7] M. Sharma, M. Olutas, A. Yeltik, Y. Kelestemur, A. Sharma, S. Delikanli, B. Guzelturk, K. Gungor, J. R. McBride, H. V. Demir, *Chem. Mater.* **2018**, *30*, 3265.
[8] K. E. Knowles, H. D. Nelson, T. B. Kilburn, D. R. Gamelin, *J. Am. Chem. Soc.* **2015**, *137*, 13138.
[9] J. Yu, M. Sharma, S. Delikanli, M. D. Birowosuto, H. V. Demir, C. Dang, *J. Phys. Chem. Lett.* **2019**, *10*, 5193.
[10] H. D. Nelson, S. O. M. Hinterding, R. Fainblat, S. E. Creutz, X. Li, D. R. Gamelin, *J. Am. Chem. Soc.* **2017**, *139*, 6411.
[11] J. Yu, C. Dang, *Cell Rep. Phys. Sci.* **2021**, *2*, 100308.
[12] P. Narayan, S. Das Adhikari, A. Nag, D. D. Sarma, *Angew. Chem., Int. Ed.* **2017**, *56*, 7038.
[13] P. Narayan, D. D. Sarma, *J. Phys. Chem. Lett.* **2011**, *2*, 2818.
[14] Y. Han, S. He, X. Luo, Y. Li, Z. Chen, W. Kang, X. Wang, K. Wu, *J. Am. Chem. Soc.* **2019**, *141*, 13033.
[15] J. Yu, M. Sharma, M. Li, P. L. Hernandez-Martinez, S. Delikanli, A. Sharma, Y. Altintas, C. Hettiarachchi, T. C. Sum, H. V. Demir, C. Dang, **2019**, *arXiv*: 1905.11571.
[16] E. Stern, R. Wagner, F. J. Sigworth, R. Breaker, T. M. Fahmy, M. A. Reed, *Nano Lett.* **2007**, *7*, 3405.

[17] J. Yu, S. Hou, M. Sharma, L. Y. M. Tobing, Z. Song, S. Delikanli, C. Hettiarachchi, D. Zhang, W. Fan, M. D. Birowosuto, H. Wang, H. V. Demir, C. Dang, *Matter* **2020**, *2*, 1550.
[18] C. Dang, J. Lee, C. Breen, J. S. Steckel, S. Coe-Sullivan, A. Nurmikko, *Nat. Nanotechnol.* **2012**, *7*, 335.
[19] S. Chen, A. Nurmikko, *Optica* **2018**, *5*, 2334.
[20] S. Chen, A. Nurmikko, *ACS Photonics* **2017**, *4*, 2486.
[21] V. Pinchetti, Q. Di, M. Lorenzon, A. Camellini, M. Fasoli, M. Zavelani-Rossi, F. Meinardi, J. Zhang, S. A. Crooker, S. Brovelli, *Nat. Nanotechnol.* **2018**, *13*, 1145.
[22] Yu, J., Sharma, M., Sharma, A., Delikanli, S., Demir, H. V., Dang, C., *Light: Sci. Appl.* **2020**, *9*, 27.
[23] B. Guzelturk, Y. Kelestemur, M. Olutas, S. Delikanli, H. V. Demir, *ACS Nano* **2014**, *8*, 6599.
[24] M. Li, M. Zhi, H. Zhu, W.-Y. Wu, Q.-H. Xu, M. H. Jhon, Y. Chan, *Nat. Commun.* **2015**, *6*, 8513.
[25] J. Yu, S. Shendre, W.-K. Koh, B. Liu, M. Li, S. Hou, C. Hettiarachchi, S. Delikanli, P. Hernández-Martínez, M. D. Birowosuto, H. Wang, T. C. Sum, H. V. Demir, C. Dang, *Sci. Adv.* **2019**, *5*, eaav3140.
[26] M. Sharma, S. Delikanli, H. V. Demir, *Proc. IEEE* **2020**, *108*, 655.